Rock Mechanics and Rock Engineering (2024) 57:2567–2580
https://doi.org/10.1007/s00603-023-03702-8

ORIGINAL PAPER

Prediction of Fracturing Pressure and Parameter Evaluations at Field Practical Scales

Lei Hou[1] · Linbo Zhou[2] · Derek Elsworth[3] · Sen Wang[4] · Wendong Wang[4]

Received: 1 June 2023 / Accepted: 26 November 2023 / Published online: 2 January 2024

Abstract

Hydraulic fracturing pressure is one of the key criteria in defining the pumping schedule and in dimensioning surface plants for fracturing operations. However, it is difficult to predict at a practical field scale due to the complex determining factors, involving geological, hydrodynamic and rock mechanical parameters. This study proposes a synthetic data-driven workflow, integrating both hydrodynamic and rock mechanical models, to predict the pressure based on fracturing experience in neighboring wells. The data quality and performance of the geological, hydrodynamic and rock mechanical features are evaluated based on a backward elimination strategy and control variate method, using error evolutions as criteria. Relatively small errors (root mean square error 5.1 ~ 5.7 MPa and mean absolute error 5.6 ~ 8.3%) are returned for wells/cases within the same region as the training wells, demonstrating the superior performance of the workflow. The prediction errors increase significantly with increasing distance between training and testing wells – defining the range of applicability of the workflow. The rock mechanical feature (represented by the brittleness index) provides a larger contribution to the prediction than that of the hydrodynamic feature (represented by the proppant accumulation) in most of the testing cases. Young's Modulus exhibits a higher performance (induces the smallest errors in pressure prediction) to characterize the rock mechanical feature of the formation, compared with the brittle mineral ratio and Poisson's Ratio. The data quality of geological stresses and Poisson's Ratio may require improvements based on the irregular error evolutions. The remaining errors and proximity/regional limitations of the data-driven workflow are critically discussed. This new method provides a platform for the prediction of pressures at field-practical scales, which may be significant for both hydraulic fracturing and geological storage of CO_2 and H_2 in depleted reservoirs with sufficient historical hydraulic fracturing records.

Highlights

- A data-driven workflow is built to predict fracturing pressure at field scales.
- Errors increase with the increasing distance between training and testing cases.
- Contribution of rock mechanical feature is larger than hydrodynamic feature.
- Young's Modulus performs better in characterizing rock mechanical feature.
- Lower data qualities of geological stresses and Poisson's Ratio are revealed.

✉ Lei Hou
leihou@sjtu.edu.cn

✉ Sen Wang
fwforest@gmail.com

[1] China-UK Low Carbon College, Shanghai Jiao Tong University, Shanghai 201306, China

[2] SINOPEC Research Institute of Petroleum Engineering, Beijing 100101, China

[3] Energy and Mineral Engineering and Geosciences, EMS Energy Institute and G3 Center, Pennsylvania State University, University Park 16802, USA

[4] School of Petroleum Engineering, China University of Petroleum (East China), Qingdao 266580, China

Keywords Hydraulic fracturing · Pressure prediction · Machine learning · Feature analyses · Case study

1 Introduction

Fracturing pressure is one of the core characterization parameters for massive hydraulic fracturing (Hou et al. 2019; Osiptsov 2017; Wang et al. 2019), especially in stimulation of unconventional reservoirs where the pressure may approach the maximum capacity of surface components (such as the capacity of the wellhead, outputs of pumps, and others), thus leaving only a narrow safety window for the hydraulic injection operation (Baumgärtner and Zoback 1989; Jarvie et al. 2007; Roussel et al. 2012; Sun et al. 2022). It continues to increase as exploration for unconventional resources ever deepens (Mou et al. 2019; Xi et al. 2021) and as well patterns become progressively denser to maintain production (Gao and Gray 2019; Zhu et al. 2021). This trend keeps challenging the use of surface equipment, the optimization of pump schedules and the safe injection of proppant – all essential concerns for pre-job design to control costs and ensure security (Nolte 1988; Qi et al. 2012). The fracturing pressure may be controlled by the rock mechanical features of formations (Hou & Elsworth 2021; Zhao et al. 2020), heterogeneous geological stresses (Gasparik et al. 2014; Wang et al. 2015; Zou et al. 2010), various injection parameters (Hu et al. 2018; Mao et al. 2021) and proppant accumulation and transport in underground fractures (Alotaibi and Miskimins 2015; Hou et al. 2017; Sahai et al. 2014; Sahai and Moghanloo 2019). Therefore, predicting the fracturing pressure at field practical scales is still challenging due to the complex determining parameters (geological, hydrodynamical, rock mechanical, and other parameters). The influence of each parameter on the fracturing pressure is also vague, especially for the rock mechanical parameters that are usually used to represent the "sweet point" and fracability, and then to optimize the fracturing strategy, such as the subsections.

Previous efforts on predictions of fracturing pressure mainly focussed on the estimation of the breakdown pressure based on experiments considering the mechanical properties of the reservoir rocks, for instance, using the limited-scale rock cylinders (5×10 cm) or blocks (30×30 cm) (Ha et al. 2018; Ma et al. 2017; Wu et al. 2020). Numerical models extend the simulation scales, however, may encounter challenges in the reduction accuracy of in situ conditions, such as the existence of natural fractures (Ma et al. 2022; Yang et al. 2022; Yuan et al. 2023). The results of these simulations typically only provide an approximate reference for the actual prototype well at scale, which is insufficient for the pre-fracturing optimization of a real treatment schedule that will typically extend over many hours. The application of data science in petroleum engineering enables the study of hydraulic fracturing at the relevant field-practical scale (Al-Anazi & Gates 2010; Lin et al. 2020; Maity and Ciezobka 2019; Zhong et al. 2020). Real-time fracturing pressures have been predicted using neural network models trained on data from the first several minutes of fracturing operations and then applied to predict the evolving pressure for the next several minutes (Ben et al. 2020). These studies mainly used hydraulic injection parameters (proppant concentration, friction reducer concentration, pump rate and wellhead pressure), which may induce bias by neglecting the rock mechanical and geological features of the fracturing well. Previous studies have also analyzed the error of the pressure predictions based on machine learning algorithms, and then to improve the expressions for the brittleness index and proppant accumulation (Hou et al. 2022b, 2022c, 2022d). However, these studies focused on one specific feature class (hydrodynamic or rock mechanics) alone, by controlling the others, which may remove certain useful information and thus induce relatively large absolute errors (~ 20%) in the prediction of pressures (Hou et al. 2022c, 2022d). Therefore, accurate predictions of fracturing pressures are still challenging.

The other challenge is to reveal the effects of geological and rock mechanical parameters on the fracturing pressure, for instance, the maximum and minimum horizontal stresses, brittleness index, mineral components, Young's Modulus and Poisson's Ratio. These parameters are usually derived from core drilling, experimental tests and well logging, both of which are costly measuring techniques (Ban et al. 2023; Haddad et al. 2023). Field engineers mainly rely on these parameters to evaluate the features of the target formation, and then make decisions on the fracturing strategy (Taghichian et al. 2018; Zhang et al. 2016). However, the derivations of these parameters are limited within (for core drilling) or around the range of wellbore (for well logging). The bias always exists due to the scale differences (between the accessed scale around wellbore and the formation scale) and the spatial heterogeneity in formation (Kolawole and Oppong 2023; Mandal et al. 2023; West and Walton 2023). Moreover, the effects of geological and rock mechanical parameters on pressure evolutions may be overshadowed by the various pump schedules which may dramatically fluctuate the fracturing pressure. Therefore, the qualities of these parameters and their contributions to the fracturing pressures are urgently to be defined at field practical scales, in order to improve both the measuring techniques and fracturing strategy in fields.

This paper proposes a data-driven workflow to predict the fracturing pressure at field engineering scales based on operational experience from neighboring wells. Both hydrodynamic and rock mechanical models are integrated into the workflow to pre-process the field data and extract input features to train a deep learning algorithm, as well as inputs of geological stresses and characteristics of the wellbore and hydraulic injection. Errors in the predictions are analyzed to demonstrate the applicability of this workflow for increasing separations from the training wells. The qualities and contributions of geological and rock mechanical features to the pressure prediction are analyzed based on error evolutions (using the backward elimination strategy and control variate method), based on which the black-box effect of the deep learning algorithm is also mitigated. This newly proposed method may significantly improve the pre-fracturing design and formation characterization for the efficiency and security of operations. Moreover, this method may also be applied to predict the injection pressure for the geological storage of CO_2 and hydrogen, to estimate the storage capacity and control any leakage induced by overpressure.

2 Methodology

We propose a machine learning (ML) based workflow to process field data from gas shale reservoir fracturing wells, which is then applied to predict the fracturing pressures for neighboring wells at various separation distances. Physics-based hydrodynamic and rock mechanical models are used to pre-process the field data and extract features as the inputs for training the ML algorithm, through which these models are integrated into the workflow. The prediction errors are analyzed to test the applicability of the new method and the contributions of various input features (geological and rock mechanical parameters).

2.1 Data Collection and Division

Field records from fractured wells in gas shale reservoirs are collected from the southeastern edge of the Sichuan basin. A square area of ~ 49 km^2 is selected and denoted as testing region X in supplying the data. The shale gas wells are drilled and fractured in the form of a multi-well pad – namely several different wells (usually 3 ~ 5 wells in region X) are drilled from the same surface location to extend horizontally in all azimuths to efficiently access the full underground reservoir. The fracturing measurements of five wells from five different pads/sites within region X are collected for training the machine learning algorithm. These include 67 stages of fracturing operations as presented in Table 1, containing 21,249 groups of data at one-minute intervals. Six more wells are set as the testing group, from which six stages of hydraulic fracturing are randomly selected. Three testing wells (X1 ~ X3) are located within region X, which are classified by the distance from the training wells. X1 and X2 are from the same pads and are defined as W1 and W2 (training wells, Table 1), respectively. X3 is from a different pad from these training wells, but is still located within region X. Correspondingly, three wells (Y1 ~ Y3) far from region X are collected for comparison. Y1 is a distant well within its region (< 50 km) close to region X. Both Y2 and Y3 are distant from (> 100 km) the training wells, as summarized in Table 1. The regional distribution of the wells is designed to test the range of the applicability of the data-driven method.

Notably, the hydraulic injection data are available at one-minute intervals and are used to train the algorithm. We use data sampled at minute resolution rather than at one-second resolution since the proposed method in this study is designed for pre-fracturing predictions. The injection parameters (mainly including the pump rate, proppant concentration, proppant and fluid types) before the fracturing operation are usually only scheduled at a single-minute resolution (Qi et al. 2012). We use the single-minute-resolution data (317 groups of data on average in each testing stage) to test the performance of the algorithm and ensure consistency in resolution between training and application data.

2.2 Data Pre-Processing

The original parameters collected from field records consist of the geological, wellbore, injection, and rock mechanical parameters. The geological category contains the principal

Table 1 Division of training and testing stages for the data-driven workflow

	Stage number	Well no	Regional	Notes
Training dataset	67 Stages	W1 ~ W5	Within region X	
Testing dataset	6 Stages (1 Stage/well)	X1		From the same pads as training wells
		X2		
		X3		From different pads
		Y1	Beyond region X	Distant well
		Y2		Far distant wells

features of the shale reservoir, including the vertical depth of the target formation, maximum and minimum horizontal stresses and pore pressures, as shown in Table 2. The well depth (length of the well trajectory), number of perforation holes and stage length are selected to represent the features of the wellbore. Hydraulic injection parameters include pump rate, viscosity and density of the mixture (proppant and fracturing fluid) and proppant diameter and concentration (Table 2). The rock mechanical parameters, used for calculating the brittleness index, include mineral composition (quartz, carbonate, clay, and total organic carbon) and mechanical properties derived from logging data (compressional slowness and porosity) and elastic properties (density, Young's modulus, and Poisson's ratio).

Both hydrodynamic (Hou et al. 2022b; Patankar et al. 2002; Wang et al. 2003) and rock mechanical models (Hou et al. 2022c) are applied to pre-process the field data, as presented in Appendix (Eqs. 1 ~ 10). The height of the slurry flowing layer within fractures (H_l) and the brittleness index of the target formations (BI) are representative features/parameters calculated by the numerical models. The use of the volume ratio of injected proppant/sand and fluid has been shown to significantly improve the prediction of ML algorithms (Hou et al. 2023) and is also included in our input features, as shown in Table 2. The friction impacting flow through the drill pipe and perforation, as well as the hydrostatic pressure of the wellbore, are also calculated based on the parameters of the hydraulic injection (Dontsov and Peirce 2014; Willingham et al. 1993) – a data augmentation method is used to improve the performance of the machine learning algorithm. The original features and hydraulic frictional losses are mainly used for training the algorithm. The extracted features of H_l and brittleness index (BI) are further analyzed to evaluate their relative contributions to predictions of fracturing pressure. The qualities and contributions of the geological (maximum and minimum horizontal stresses) and rock mechanical features (brittle mineral ratio – proportion of quartz and carbonate, Young's Modulus and Poisson's Ratio) are also evaluated based on the control variate method.

2.3 Machine Learning Workflow and Algorithm Tuning

An ML-based workflow is established to process the field data and produce the prediction of fracturing pressures at field engineering scales, as presented in Fig. 1. The Gated Recurrent Unit (GRU) algorithm, designed for the processing of time-sequential data, is used for data processing, as based on previous experience (Hou et al. 2022a, 2023), which

Table 2 Summary of the original and extracted features based on field records and numerical models

		Inputs to ML Algorithm	Output
Original features	Geological	Vertical depth of formation; Maximum and minimum horizontal stresses; Pore pressure	Wellhead pressure
	Wellbore	Well depth; Number of perforation holes; Stage length	
	Injection	Pump rate; Mixture viscosity; Mixture density; Proppant diameter and concentration; V_s/V_f	
Extracted features	Hydro-dynamics	Pipe and perforation Frictions; Hydrostatic pressure	
		H_l	
	Rock mechanics	BI	

V_s/V_f – the volume ratio of injected proppant and fluid; H_l – the height of the slurry flowing layer in fractures; BI – brittleness index, calculated by combining brittle mineral ratio, Young's modulus and Poisson's ratio. The parameters for evaluations include H_l and BI, geological stresses, brittle mineral ratio, Young's modulus and Poisson's ratio

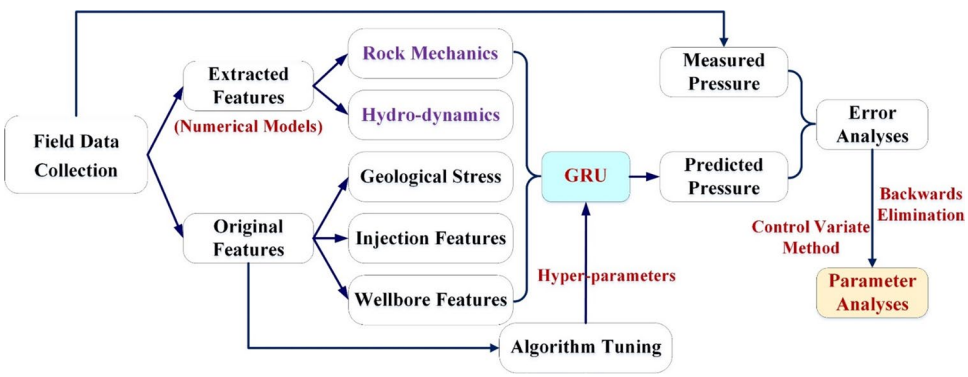

Fig. 1 Structure of the data-driven workflow for predictions of hydraulic fracturing

is the pivot of the workflow (as highlighted in Fig. 1). The hyperparameters of the GRU are optimized to improve its performance based on tuning of the algorithm. The numerical models (Eqs. 1 ~ 10, Appendix) are integrated into the workflow for feature extractions and data pre-processing. Both the root mean squared error (RMSE) and mean absolute error (MAE) are used in evaluating the correspondence of the predicted pressure relative to the field measurements. The backward elimination strategy and control variate method are deployed to analyze the contribution of individual features, during which one feature at-a-time is sequentially eliminated. The error evolutions due to the tested feature are then used as the criterion for parameter analyses.

The GRU model with 3 layers (including the output layer) is built to predict the fracturing pressure, as based on previous experience (Hou et al. 2022a, 2023). A drop-out (drop rate is 0.1) layer is set after the first and hidden layers, respectively, to avoid overfitting. The activation function ('ReLu') and optimizer ('Adam') are designed for the continuous output of pressures (Gal & Ghahramani 2015; Kingma & Ba 2014). The hyperparameters of the GRU algorithm are optimized by combining the grid search and walk-forward validation techniques (Bergstra & Bengio 2012; Hu et al. 1999). The candidate hyperparameters are the neural nodes in each layer [50, 100, 200], the epochs [20, 40] and the batch size [50, 100, 150]. A total of 18 combinations of the hyperparameters are set for tuning the deep learning algorithm. RMSE is used as the criterion for optimization, which has the same unit (MPa) as the prediction. The errors based on different combinations are summarized in Table 3. The root mean square error (RMSE) of the fracturing pressure approaches a minimum value of ~ 3.30 MPa based on the combination [200, 20, 150] for the neural nodes in each layer, epochs and batch size, respectively, which are used for the hyperparameters of the GRU algorithm.

3 Results

The optimized GRU algorithm (Table 3) produces a prediction of fracturing pressures based on the input features (Table 2) from region X (Table 1). The results are presented in Figs. 2 and 3. In general, the deviations between predicted pressures and measured pressures are much smaller in cases within the same region as the training wells. The close locations between these testing and training wells may constrain the geological uncertainties and then mitigate errors in the predictions. The predicted pressure varies around the measurements in Fig. 2, showing relatively small errors in predictions. X1 and X2 are the same-pads wells as the training wells, and X3 is a neighbor well within region X. The RMSE in the nearby cases varies between 5.1 MPa and 5.7 MPa (5.3 MPa on average), and the MAE varies between 5.6% and 8.3% (6.9% on average), which demonstrates the performance of the machine learning workflow.

However, the applicability of this data-driven method should be restricted to within the same region as the training wells (region X) since the performance of the ML-based workflow decreases for cases far from the training wells (beyond region X), as shown in Fig. 3. Apparent deviations are observed between predictions and field-measured pressures, which increase with increasing distance between the training and testing wells, as apparent in the deviations in Y1 (< 50 km) and Y2 and Y3 (> 100 km). The shale formation is relatively continuous between the training wells and Y1 next to region X. The formation containing Y2 and Y3, distant from region X, however, is geologically disconnected by faulting and folding. Different subsurface conditions may result in large errors between predictions and measurements. Noteworthy, the patterns (variations and trends) of predicted pressure curves are similar to the field records. Specifically, the pressure variations earlier than 100 min into the stimulation (Fig. 3) are mainly induced by pump rate adjustments, which are recognized by the trained algorithm and thus predict similar fluctuations in pressures compared with field records.

This new method is especially useful for multi-well pad fracturing, during which the fracturing pressure of target wells may be predicted by prior experience from fracturing adjacent wells from the same or neighboring pads. Then, the parameters of hydraulic injection (proppant volume, fluid viscosity, and others) may be optimized for higher fracturing efficiency and better stimulation results. This new workflow

Table 3 Summary of results for algorithm tuning

Tested hyperparameters	RMSE/MPa	Tested hyperparameters	RMSE/MPa	Tested hyperparameters	RMSE/MPa
50, 20, 50	8.18	50, 20, 100	8.18	50, 20, 150	8.18
50, 40, 50	8.14	50, 40, 100	4.22	50, 40, 150	8.18
100, 20, 50	8.18	100, 20, 100	4.03	100, 20, 150	5.50
100, 40, 50	4.94	100, 40, 100	4.21	100, 40, 150	6.33
200, 20, 50	4.43	200, 20, 100	3.57	200, 20, 150	3.30
200, 40, 50	3.72	200, 40, 100	4.50	200, 40, 150	3.73

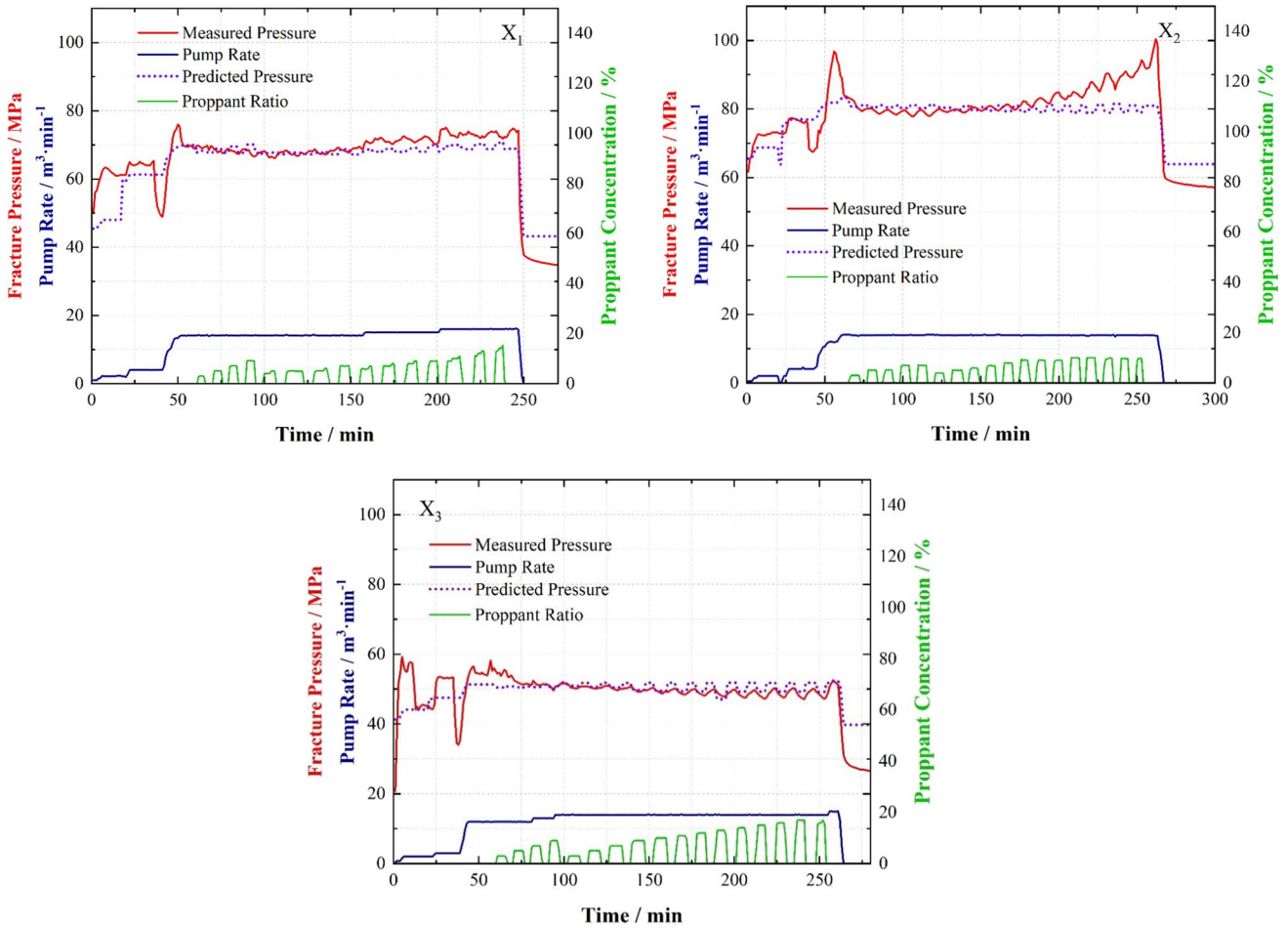

Fig. 2 Predictions of fracturing pressures and field measurements of **a** well X1, **b** well X2 and **c** well X3 within region X

can also be significant for fracturing the infilled wells that are drilled between the pattern of previously fractured wells. The prior fracturing records provide useful data in training the GRU algorithm that is then applied to predict the required/desired operational pressures for the new infilled wells. Moreover, this new strategy may also be useful for predicting the injection pressure for CO_2 and hydrogen storage in depleted oil and gas reservoirs, with a sufficient documented history of previously fractured wells.

4 Discussion

The data-driven workflow is further applied for sensitivity analyses using the prediction errors as criteria. Different input combinations are designed in the workflow based on the backward elimination strategy and control variate method, as presented in Table 4. The parameter's quality and contribution to pressure prediction are analyzed based on the error evolutions resulting from different input combinations in the training and prediction algorithms. This also mitigates the "black-box effect" by illuminating the internal characteristics of the deep learning algorithm. The results are summarized in Table 4, where both RMSE and MAE are used for error analyses. Six groups of errors are generated from all testing wells (X1 ~ X3 and Y1 ~ Y3) based on seven groups of combinations of input features. The all-features combination (Table 4) synthesizes the errors in Figs. 2 and 3, which are used as a lower-limit reference.

The maximum and minimum stress, H_1 and BI are excluded one at a time from the inputs of the training and testing datasets to compare the error evolutions – the backward elimination strategy (Table 4). The larger induced error indicates a more significant contribution of the eliminated feature to the fracturing pressure. In contrast, the larger induced error indicates a lower quality/performance of the tested parameter using the control variate method (Table 4). This method replaces BI successively by the brittle mineral ratio (proportion of quartz and carbonate, Eq. 6 in Appendix), Young's Modulus and Poisson's Ratio, to test the quality and performance of the representative rock mechanical parameters in fields. The replacement strategy is applied to

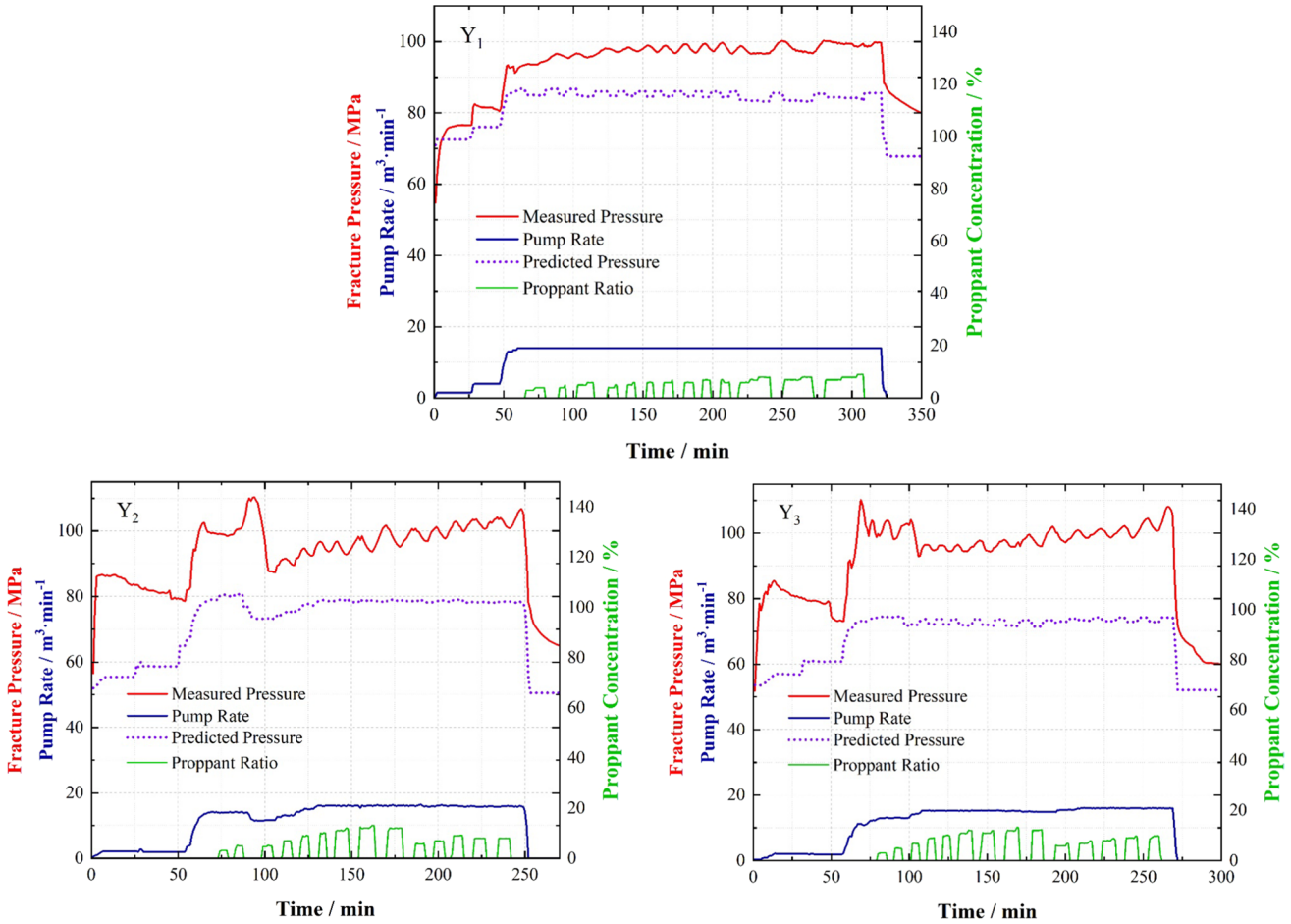

Fig. 3 Predictions of fracturing pressures and field measurements of wells beyond region X. **a** Y1 is a distant well next to region X (<50 km); **b** Y2 and **c** Y3 are wells distant (> 100 km) from region X

mitigate the parametric interference because the *BI* (calculated by Eqs. 5 and 6 in the Appendix) involves all of the tested parameters. In general, lower errors are reported in the backward-elimination group (using extracted features) than the errors in the control-variate group (using original parameters), which indicates the importance of the integrated numerical models. The elimination of *BI* generates the largest errors in most cases in the backward-elimination group, which demonstrates the largest contribution of *BI*. In contrast, the larger errors induced by Poisson's Ratio indicate its lower quality and performance compared with the brittle mineral ratio and Young's Modulus.

4.1 Comparison Between Hydrodynamic and Rock Mechanical Features

The proppant accumulation in fractures (H_1) and brittleness index of formation (*BI*) are selected as the representative hydrodynamic and rock mechanical features for comparison. The evolutions of RMSE and MAE excluding H_1 and *BI* are compared in Fig. 4. Both of the errors increase relative to the lower reference limit based on all features. Similar trends in variation are observed in RMSE and MAE curves. Larger increases in error are obtained for far-distant cases (Y2 and Y3) beyond region X, compared with the increases in error for cases within (X1 ~ X3) and close to (Y1) region X. However, both increasing and decreasing trends in errors are observed due to the feature eliminations in nearby cases (X1 ~ X3). A single error-increasing trend is obtained in distant cases (Y1 ~ Y3), in which both RMSE and MAE are one magnitude larger than the errors in nearby cases.

The evolution of RMSE is furthermore analyzed to define the contributions of the hydrodynamic (H_1) and rock mechanical (*BI*) features to the predictions of fracturing pressures, as shown in Fig. 5. Generally, the growth rates of RMSE are larger when eliminating the *BI* (the red bar in Fig. 5) than the rates when eliminating the H_1 (the blue bar in Fig. 5). The larger growth rates of errors (~60%) indicate the greater importance of *BI* in the predictions, compared with the H_1 (~25% of the growth rate of errors). Notably, a

Table 4 Summary of error evolutions for parameter evaluations

Well No	Errors	All features	Backward elimination strategy*			Control variate method**		
			Eliminate stresses	Eliminate H_1	Eliminate *BI*	Brittle mineral ratio	Young's modulus	Poisson's ratio
X 1	RMSE	5.122	5.74	5.18	8.151	9.831	6.315	29.074
	MAE	0.067	0.082	0.053	0.107	0.131	0.094	0.481
X 2	RMSE	5.694	10.17	7.09	7.912	11.047	7.45	31.344
	MAE	0.056	0.113	0.07	0.079	0.125	0.074	0.414
X 3	RMSE	5.122	5.026	6.049	4.793	4.409	4.546	22.986
	MAE	0.083	0.081	0.112	0.084	0.069	0.074	0.504
Y1	RMSE	12.054	17.717	13.323	16.233	19.738	15.87	22.96
	MAE	0.122	0.185	0.136	0.168	0.208	0.163	0.248
Y2	RMSE	21.045	15.188	24.145	27.364	30.926	24.073	13.362
	MAE	0.226	0.153	0.266	0.305	0.342	0.259	0.145
Y3	RMSE	23.277	16.401	26.033	29.564	32.457	27.614	10.463
	MAE	0.242	0.162	0.291	0.329	0.356	0.293	0.106

*Geological stresses, H_1 and *BI* are evaluated by eliminating them one at a time from the inputs – a backward elimination strategy. The larger induced error by the tested parameter indicates a more significant contribution to pressure prediction

**The brittle mineral ratio, Young's modulus and Poisson's ratio are used, one at a time, to replace the *BI*. Other inputs are set as the control variables to compare the error evolutions– the control variate method. The small error by the tested parameter indicates a higher performance to characterize the rock mechanical feature of the formation

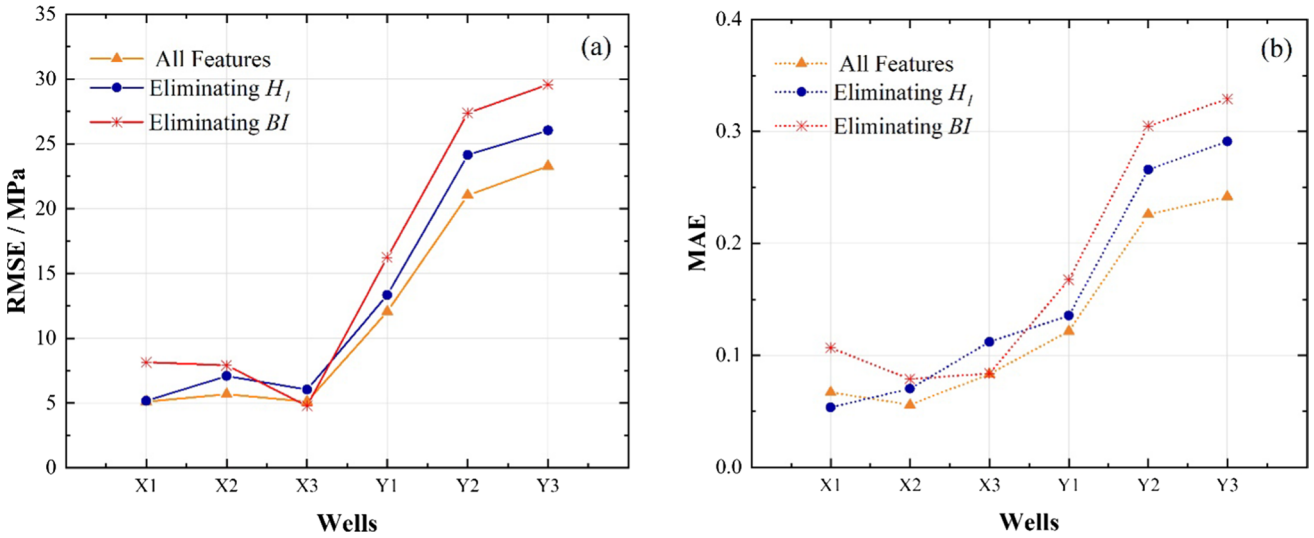

Fig. 4 Increases in **a** RMSE and **b** MAE by excluding the hydrodynamic (H_1) and rock mechanical (*BI*) features from the inputs

negative growth rate in the error is reported in the case of X3 after the *BI* is excluded from the inputs, which indicates that the *BI* induces extra error when predicting the fracturing pressure. This anomalous evolution may be explained by the presence in the reservoir of fully developed fractures with sufficient width to accommodate proppant injection. Thus, the behavior of proppant transport (represented by H_1 in this study) may dominate the pressure variation rather than the propagation of the fracture (*BI*) and thus be reflected in the prediction of pressures. The lowest fracturing pressure (~ 50 MPa) and declining trend of the pressure curve in the case of X3 bolsters this interpretation, as shown in Fig. 2 (c).

4.2 Performance of Geological Stresses

The evolution of RMSE and MAE, excluding geological stresses (the maximum and minimum horizontal stresses) from input features, are shown in Fig. 6. The effects of

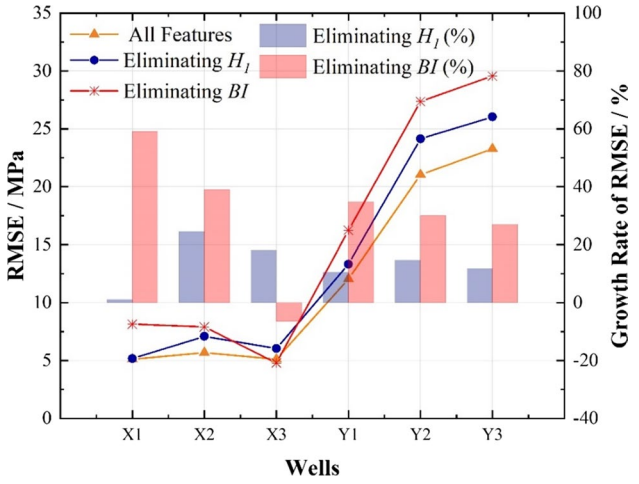

Fig. 5 Growth rate of RMSE in the field cases with a single hydrodynamic or rock mechanical feature

geological stresses on prediction errors are irregular. Only small errors are generated after eliminating stresses in cases of X1 and X3. Significant increases in error are observed in X2 and Y1. However, errors for far-distant cases (Y2 and Y3) decrease after the eliminations, indicating an interference characteristic of stresses in Y2 and Y3. The minimum horizontal stresses are also drawn in Fig. 6, which are usually used to evaluate fracture propagation pressures (Hu et al. 2019; Huang et al. 2019). High stresses are reported in X1, Y2 and Y3, but opposite trends in error evolution are observed in these cases, which exclude the dominant influence of stress difference. This anomalous phenomenon may result from difficulties in the accurate recognition of heterogeneous geological stresses. Moreover, the in-situ stresses recovered from the fracturing wells are usually assumed for neighboring wells as this saves the cost of additional well-logging, especially for production wells. This may furthermore generate uncertainties in characterizing the in situ stresses, which constrains the data quality of stresses for predictions. In contrast, the spatial neighborhood between training wells and X1 ~ X3 within region X may constrain geological variations and uncertainties, which results in more accurate predictions (Fig. 3) and regularized rules for error evolution (Fig. 4).

4.3 Evaluations of Rock Mechanical Parameters

The data quality and performance of the key rock mechanical parameters are evaluated and compared, mainly including the brittle mineral ratio (proportion of quartz and carbonate), Young's Modulus and Poisson's Ratio. The error evolution with a single rock mechanical parameter (by controlling other original and extracted features, Table 2) is used as the criterion for evaluation. The *BI*, involving all these parameters (Eqs. 5 and 6, Appendix), is replaced by the testing parameter, one at a time, to avoid parametric interference. The results of the error evolution are presented in Fig. 7. Larger induced error indicates a lower data quality or performance of the corresponding rock mechanical parameter. Generally, a similar evolution trend is obtained in error evolution curves of the groups of all-feature, brittle-mineral-ratio and Young's-Modulus. Young's Modulus induces the smallest errors in most of the cases (except for the X3 case), indicating the most significant contribution of Young's Modulus in pressure prediction, as well as its performance in characterizing the rock mechanical feature of the formation. Meanwhile, a decreasing error evolution curve, opposite to all other three increasing-trend curves, is observed in the Poisson's-Ratio group. The Poisson's Ratio and Young's Modulus are paired parameters and usually are derived from well-logging or rock mechanical tests of the

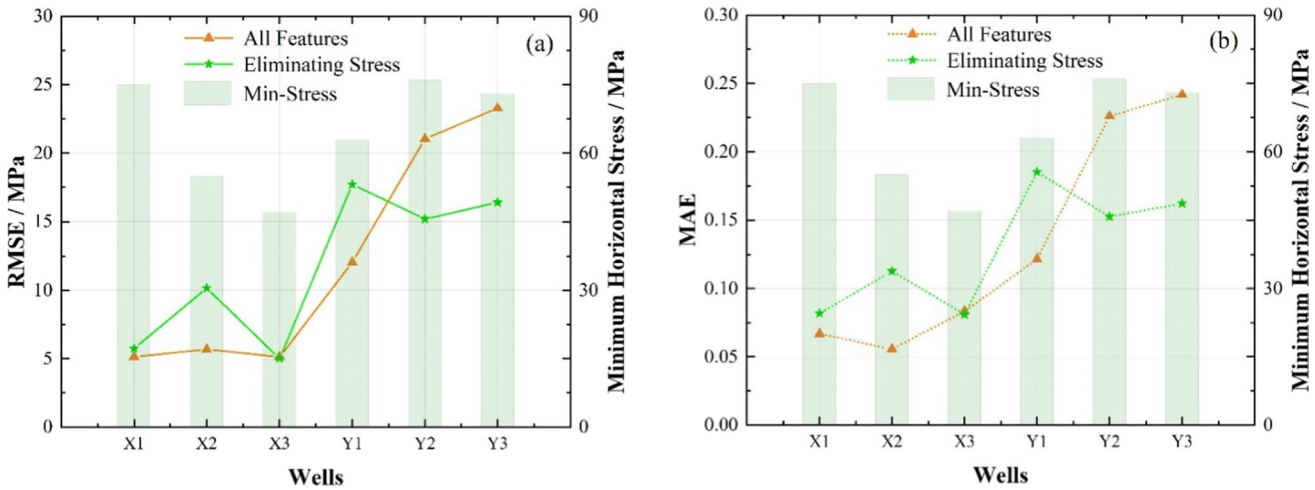

Fig. 6 Evolution of **a** RMSE and **b** MAE by eliminating geological stresses (the maximum and minimum horizontal stresses) from inputs

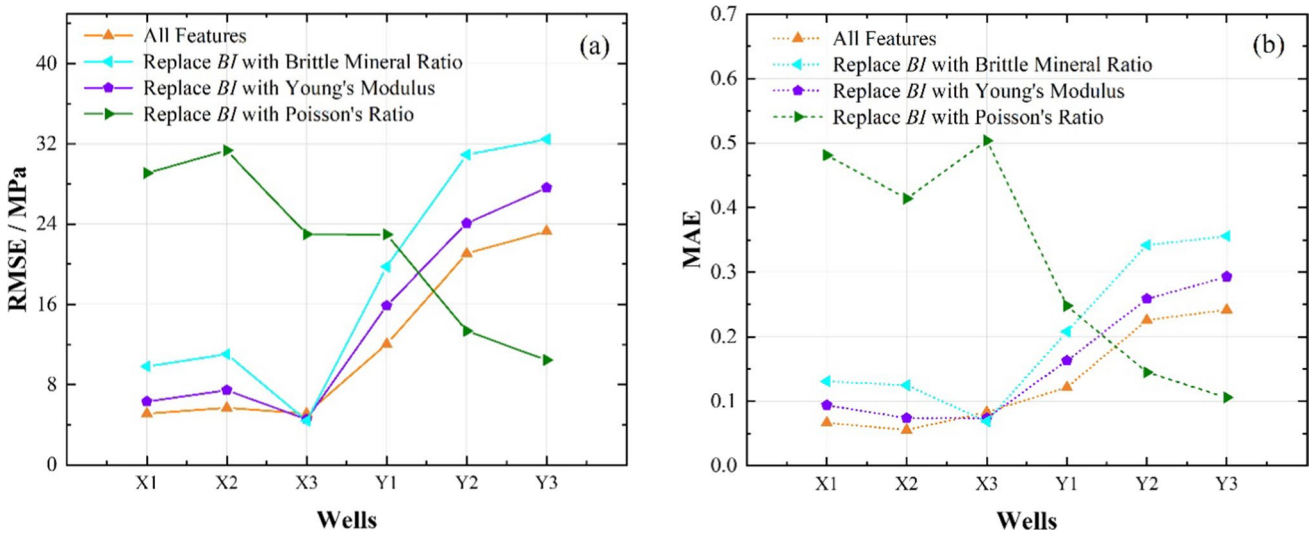

Fig. 7 Evolutions in **a** RMSE and **b** MAE with a single rock mechanical parameter (the brittle mineral ratio, Young's Modulus and Poisson's Ratio) and controlling other input features

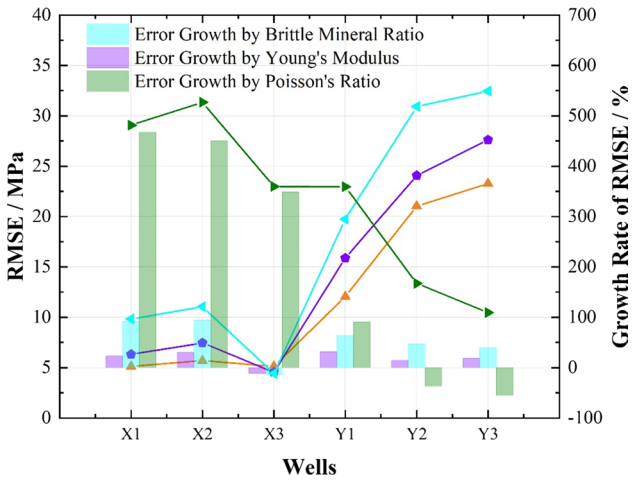

Fig. 8 Growth rate of RMSE in field cases with a single rock mechanical parameter, involving the brittle mineral ratio, Young's Modulus and Poisson's Ratio

drilled core. The irregular error evolution in the Poisson's-Ratio group may be caused by the lower data quality, which may require improvements in evaluating technique.

The evolution of RMSE is furthermore analyzed to evaluate the data quality and the contribution of each rock mechanical parameter to pressure prediction, as shown in Fig. 8. The smallest growth rates of errors (~32%) indicate the greater importance of the Young's Modulus in the predictions, compared with the brittle mineral ratio (~94%) and the Poisson's Ratio (~468% of the growth rate of errors). The abnormal negative growth rate in errors in the X3 case is explained by the same reason as the observation in Fig. 5. The hydrodynamic feature may dominate the fracturing pressure, and the introduction of rock mechanical features may induce extra errors. In the Poisson's Ratio group, significant increases in errors are observed in the nearby cases (X1 ~ X3). However, the errors in the far-distant cases (Y2 and Y3) are approximately halved by Poisson's Ratio. This is because the predicted pressures in all six cases with a single Poisson's Ratio are much larger than the predictions with a single brittle mineral ratio or Young's Modulus, as presented in Figs I, II and III in Appendix. These positive deviations result in large error increases in nearby cases with lower field-measured pressures. However, these may diminish the errors, by coincidence, in far-distant cases with high-level pressures. The failures in predicting the pressure trends are observed before 100 min in cases of Y2 and Y3 (Fig. III). To sum up, Young's Modulus exhibits a higher performance to characterize the rock mechanical feature of the formation. The improvement in the data quality of Poisson's Ratio may be crucial according to its limited contribution to pressure predictions.

5 Limitations and Implications

5.1 Remaining Errors in Cases within Region X

The remaining errors in cases within region X (Fig. 2) are mainly present at the initiation (~50 min) of fracturing operations when pure fluids are initially injected and the pressures fluctuate dramatically due to the generation of the initial fracture networks. The heterogeneity of rock mechanical properties and geological conditions may be dominant,

at this time, but requires more and separate investigation to confirm – and thus is beyond the scope of this study. Moreover, randomly present, reactivated and opening fractures generate extra uncertainties in the prediction of pressures (Baldini et al. 2018; Merry & Dalamarinis 2020). Additionally, the clogging of the formation by drilling fluids near the wellbore may also reduce the permeability of the formation and result in anomalous high-fracturing pressures. Mineral acids (usually HCL) are often injected at the beginning of fracturing operations to remove plugging and "skin" present in the near-wellbore, which may also reduce the breakdown pressure of the formation (Guo et al. 2017). The pressure may drop rapidly and significantly as the acid approaches the formation, which is difficult to recognize and be learned by the algorithm and thus potentially generates additional errors. The deviation between predictions and records at the end of X2 (~ 250 min) may result from the use of large-size proppant (30/50 mesh) that is relatively rare in region X, which may be ignored by the algorithm because of the limited learning samples/data and thereby contribute to a local increase in error.

The other reason for the remaining error is due to information loss through the use of only minute-resolution interval data. The injection information is compressed to the minute interval level by simple decimation, resulting in the loss of 59 data points per minute compared with second-based resolution interval data. The corresponding results can be observed apparently in the capped and rectangular pressure variations of the predictions compared with the smooth and continuous records of the actual pumping data, as shown at the end of operations (~ 225 min) in Fig. 2 (b) and (c). However, we use minute-resolution data rather than second-resolution to maintain consistency between training and application data when we use this method for pre-fracturing design (during which the pump schedule is usually at the minute-interval-resolution) (Qi et al. 2012). Although rectified and coarse during fracturing, the deviations between field pressure records and predictions are small, indicating a relatively high accuracy that will benefit the pre-fracturing design. Moreover, the prediction errors can be improved by continuously updating the algorithm with new data, which is the very essence of the data-driven method (Goodfellow et al. 2016).

5.2 Regional Limitations of the Data-Driven Method

The data-driven method proposed in this study may be effectively used to predict the fracturing pressure for wells located in the same region as the training wells. The applicability of this new method should follow this regional limitation to constrain the impact of geological uncertainties and ensure the performance of the machine learning algorithm. The applicable range of this method may depend on the requirement of accuracy, based on the rule that the prediction error increases with increasing distance between the training and subject/prediction wells. Therefore, this new method may be most useful for the intensive development of gas shale fields with a sufficient documented history of previously fractured wells. For instance, the fracturing operation for an infill well that is drilled between an existing well pattern, as well as for multi-well-pad fracturing may benefit from the best predictions. The developments of infill wells and multi-well-pad fracturing are currently essential strategies used to maintain shale gas production in the southeastern Sichuan basin and elsewhere. This new strategy may also be applicable for the prediction of injection pressures for CO_2 and hydrogen storage by learning the hydraulic fracturing history of the depositing formation.

6 Conclusions

A synthetic data-driven workflow is proposed to process field data from shale gas fracturing wells and to predict the fracturing pressure of new wells by learning from the operational experience of neighboring wells. A GRU algorithm is applied in this workflow, for which the hyperparameters are optimized by combining grid search and walk-forward validation techniques. Numerical models are also integrated into the workflow for data pre-processing, which significantly improves the accuracy of prediction. The importance of geological and rock mechanical features is analyzed at field practical scales based on the increased errors induced by the individual and successive elimination of corresponding features. This data-driven workflow predicts the hydraulic injection pressure at field-practical scales for pre-fracturing design – especially useful in fracturing on multi-well pads and for infilled wells and may be also useful for predicting the injection pressure for geological storage of CO_2 and hydrogen. The major conclusions are generalized as:

(1) The deviations between predicted pressures and field records are relatively small in cases from the same region as the training wells – resulting in small errors in RMSE (5.1 MPa ~ 5.7 MPa) and MAE (5.6% ~ 8.3%). The predictions, therefore, can be used as an important reference in the pre-fracturing design of pump schedules and dimensioning of surface equipment. The errors, however, increase significantly with increasing separation between training and testing wells, which are ~ 5 times larger than errors for wells within the same region. The heterogeneity of geological conditions (currently difficult to precisely characterize) may constrain the performance of the algorithm. Therefore, the applicability of this data-driven method is recom-

mended to be restricted within the same region as the training data source;

(2) The contribution of rock mechanical features (represented by *BI*) is more significant than the contribution of hydrodynamic features (represented by H_1) to the fidelity of the predictions in most of the testing cases, based on the larger increases in RMSE when eliminating *BI*. However, an anomalous decrease in RMSE is reported in the case of X3 (Fig. 5), indicating an interference characteristic of *BI*. This may be attributed to the potential reactivation or opening of fracture networks with sufficient fracture width and volume to readily accept proppant. The fracturing pressure, therefore, mainly reflects the proppant accumulation and variation (represented by H_1) in fractures, which forestalls the effect of *BI* on the prediction of pressures. The lowest fracturing pressure and a declining trend of the pressure history in the case of X3 (as presented in Fig. 2) bolster such an interpretation;

(3) Anomalously decreasing errors are reported for increasingly distant wells (> 100 km as in Y2 and Y3) when eliminating the maximum and minimum horizontal stresses from the input features – thus indicating the interference characteristics of stresses for these cases. The high heterogeneity and low quality of the data characterizing the in situ stresses may induce extra errors. For instance, the measured stresses of neighboring pre-fractured wells are often applied directly to represent the stress condition of the new wells for cost savings. Therefore, advances in well-logging and interpretation techniques are urgent to control the investment and promote the data quality of stresses;

(4) The performance of the most commonly used rock mechanical parameters is evaluated based on the control variate method. Young's Modulus induces the smallest errors in most cases (~32% of the growth rate of errors compared with the error using *BI* as the input feature), followed by the brittle mineral raito (~94% of the growth rate) and Poisson's Ratio (468% of the growth rate), which indicates a higher performance of Young's Modulus to characterize the rock mechanical feature of the formation. An abnormal decreasing error evolution trend, along with the increasing distance between training and testing wells, is observed using Poisson's-Ratio as the input feature. This decreasing trend is opposite to the trend of error evolution curves based on all other inputs, which indicates a lower data quality of Poisson's Ratio that may require improvements.

Supplementary Information The online version contains supplementary material available at https://doi.org/10.1007/s00603-023-03702-8.

Acknowledgements This research is funded by the National Natural Science Foundation of China under grant 42377138.

Author Contributions LH: Conceptualization, Methodology, Writing-Original draft, Investigation, Revision. LZ: Data Collection, Investigation. DE: Conceptualization, Methodology, Writing-Reviewing. SW: Investigation, Methodology, Revision. WW: Data Collection, Editing.

Funding The authors are grateful to National Natural Science Foundation of China (NSFC) via a project: No. 42377138.

Data Availability Data of figures and tables presented in the current study are available from the corresponding author upon reasonable request. The training dataset for algorithm training was used under license for the current study. Restrictions are applied to the availability of these data, and so are not publicly available.

Declarations

Conflict of Interest The authors declare that they have no known competing financial interests or personal relationships that could have appeared to influence the work reported in this paper.

References

Al-Anazi A, Gates I (2010) A support vector machine algorithm to classify lithofacies and model permeability in heterogeneous reservoirs. Eng Geol 114(3–4):267–277

Alotaibi MA, Miskimins JL (2015) Slickwater proppant transport in complex fractures: new experimental findings & scalable correlation. SPE Ann Tech Conf Exhib. https://doi.org/10.2118/174828-MS

Baldini M, Carlevaro CM, Pugnaloni LA, Sánchez M (2018) Numerical simulation of proppant transport in a planar fracture. A study of perforation placement and injection strategy. Int J Multiph Flow 109:207–218. https://doi.org/10.1016/j.ijmultiphaseflow.2018.08.005

Ban L, Wang Z, Du W, Hou Y, Qi C, Yu J (2023) Investigation on the physical mechanism of cavity percentage dependent shear strength for rock joints considering the real contact joint surface. Rock Mech Bull 2(4):100064. https://doi.org/10.1016/j.rockmb.2023.100064

Baumgärtner J, Zoback MD (1989) Interpretation of hydraulic fracturing pressure-time records using interactive analysis methods [Article]. Int J Rock Mech Min Sci 26(6):461–469. https://doi.org/10.1016/0148-9062(89)91422-8

Ben Y, Perrotte M, Ezzatabadipour M, Ali I, Sankaran S, Harlin C, Cao D (2020) Real time hydraulic fracturing pressure prediction with machine learning. SPE Hydraul Fract Technol Conf Exhib. https://doi.org/10.2118/199699-MS

Bergstra J, Bengio Y (2012) Random search for hyper-parameter optimization. J Mach Learn Res 13(2):281–305

Dontsov EV, Peirce AP (2014) Slurry flow, gravitational settling and a proppant transport model for hydraulic fractures. J Fluid Mech 760:567–590. https://doi.org/10.1017/jfm.2014.606

Gal Y, Ghahramani Z (2015). A theoretically grounded application of dropout in recurrent neural networks. arXiv preprint arXiv:1512.05287

Gao C, Gray K (2019) A workflow for infill well design: wellbore stability analysis through a coupled geomechanics and reservoir simulator. J Petrol Sci Eng 176:279–290

Gasparik M, Bertier P, Gensterblum Y, Ghanizadeh A, Krooss BM, Littke R (2014) Geological controls on the methane storage

capacity in organic-rich shales. Int J Coal Geol 123:34–51. https://doi.org/10.1016/j.coal.2013.06.010
Goodfellow I, Bengio Y, Courville A (2016). Deep learning. MIT press
Guo T, Li Y, Ding Y, Qu Z, Gai N, Rui Z (2017) Evaluation of acid fracturing treatments in shale formation. Energy Fuels 31(10):10479–10489
Ha SJ, Choo J, Yun TS (2018) Liquid CO 2 fracturing: Effect of fluid permeation on the breakdown pressure and cracking behavior. Rock Mech Rock Eng 51(11):3407–3420
Haddad M, Ahmadian M, Ge J, Nicot JP, Ambrose W (2023) Geomechanical and hydrogeological evaluation of a shallow hydraulic fracture at the devine fracture pilot site, Medina county. Texas Rock Mech Rock Eng 56(10):7049–7069. https://doi.org/10.1007/s00603-022-03115-z
Hou L, Elsworth D (2021) Mechanisms of tripartite permeability evolution for supercritical CO2 in propped shale fractures. Fuel. https://doi.org/10.1016/j.fuel.2021.120188
Hou L, Jiang T, Li G, Zeng Y, Cheng Y (2017) The key parameters of proppant transport in complex fractures. Chin Sci Bull 62(26):3112–3120. https://doi.org/10.1360/n972016-00814
Hou B, Chang Z, Fu W, Muhadasi Y, Chen M (2019) Fracture initiation and propagation in a deep shale gas reservoir subject to an alternating-fluid-injection hydraulic-fracturing treatment. SPE J 24(04):1839–831855
Hou L, Cheng Y, Elsworth D, Liu H, Ren J (2022a) Prediction of the continuous probability of sand screenout based on a deep learning workflow. SPE J. https://doi.org/10.2118/209192-pa
Hou L, Cheng Y, Wang X, Ren J, Geng X (2022b) Effect of slickwater-alternate-slurry injection on proppant transport at field scales: a hybrid approach combining experiments and deep learning. Energy. https://doi.org/10.1016/j.energy.2021.122987
Hou L, Ren J, Fang Y, Cheng Y (2022c) Data-driven optimization of brittleness index for hydraulic fracturing. Int J Rock Mech Min Sci. https://doi.org/10.1016/j.ijrmms.2022.105207
Hou L, Wang X, Bian X, Liu H, Gong P (2022d) Evaluating essential features of proppant transport at engineering scales combining field measurements with machine learning algorithms. J Nat Gas Sci Eng. https://doi.org/10.1016/j.jngse.2022.104768
Hou L, Elsworth D, Zhang F, Wang Z, Zhang J (2023) Evaluation of proppant injection based on a data-driven approach integrating numerical and ensemble learning models. Energy. https://doi.org/10.1016/j.energy.2022.126122
Hu MY, Zhang G, Jiang CX, Patuwo BE (1999) A cross-validation analysis of neural network out-of-sample performance in exchange rate forecasting. Decis Sci 30(1):197–216
Hu X, Wu K, Li G, Tang J, Shen Z (2018) Effect of proppant addition schedule on the proppant distribution in a straight fracture for slickwater treatment. J Petrol Sci Eng 167:110–119. https://doi.org/10.1016/j.petrol.2018.03.081
Hu X, Liu G, Luo G, Ehlig-Economides C (2019) Model for asymmetric hydraulic fractures with nonuniform-stress distribution. SPE Prod Oper. https://doi.org/10.2118/195193-pa
Huang J, Morris JP, Fu P, Settgast RR, Sherman CS, Ryerson FJ (2019) Hydraulic-fracture-height growth under the combined influence of stress barriers and natural fractures. SPE J 24(01):302–318. https://doi.org/10.2118/189861-pa
Jarvie DM, Hill RJ, Ruble TE, Pollastro RM (2007) Unconventional shale-gas systems: the Mississippian Barnett Shale of north-central Texas as one model for thermogenic shale-gas assessment [Article]. Am Asso Petrol Geol Bull 91(4):475–499. https://doi.org/10.1306/12190606068
Kingma DP, Ba J (2014). Adam: A method for stochastic optimization. arXiv preprint arXiv:1412.6980
Kolawole O, Oppong F (2023) Assessment of inherent heterogeneity effect on continuous mechanical properties of shale via uniaxial compression and scratch test methods. Rock Mech Bull 2(4):100065. https://doi.org/10.1016/j.rockmb.2023.100065
Lin H, Kang W-H, Oh J, Canbulat I (2020) Estimation of in-situ maximum horizontal principal stress magnitudes from borehole breakout data using machine learning. Int J Rock Mech Min Sci 126:104199
Ma T, Wu B, Fu J, Zhang Q, Chen P (2017) Fracture pressure prediction for layered formations with anisotropic rock strengths. J Nat Gas Sci Eng 38:485–503. https://doi.org/10.1016/j.jngse.2017.01.002
Ma X, Zhang S, Zhang X, Liu J, Jin J, Cheng W, Jiang W, Zhang G, Chen Z, Zoback MD (2022) Lithology-controlled stress variations of longmaxi shale – example of an appraisal wellbore in the Changning area. Rock Mech Bull 1(1):100002. https://doi.org/10.1016/j.rockmb.2022.100002
Maity D, Ciezobka J (2019) Designing a robust proppant detection and classification workflow using machine learning for subsurface fractured rock samples post hydraulic fracturing operations. J Petrol Sci Eng 172:588–606
Mandal PP, Sarout J, Rezaee R (2023) Triaxial deformation of the goldwyer gas shale at in situ stress conditions—part ii: viscoelastic creep/relaxation and frictional failure. Rock Mech Rock Eng 56(10):7441–7474. https://doi.org/10.1007/s00603-023-03437-6
Mao S, Siddhamshetty P, Zhang Z, Yu W, Chun T, Kwon JS-I, Wu K (2021) Impact of proppant pumping schedule on well production for slickwater fracturing. SPE J 26(01):342–358. https://doi.org/10.2118/204235-pa
Merry H, Dalamarinis P (2020). Multi-basin case study of real-time perforation quality assessment for screen out mitigation and treatment design optimization using tube wave measurements. spe annual technical conference and exhibition
Mou Y, Lian Z, Sang P, Yu H, Zhang Q, Li R (2019) Study on water hammer effect on defective tubing failure in high pressure deep gas well. Eng Fail Anal 106:104154
Nolte K (1988) Principles for fracture design based on pressure analysis. SPE Prod Eng 3(01):22–30
Osiptsov AA (2017) Fluid mechanics of hydraulic fracturing: a review. J Petrol Sci Eng 156:513–535
Patankar NA, Joseph D, Wang J, Barree R, Conway M, Asadi M (2002) Power law correlations for sediment transport in pressure driven channel flows. Int J Multiph Flow 28(8):1269–1292
Qi W, Yun X, Xiaoquan W, Tengfei W, Zhang S (2012) Volume fracturing technology of unconventional reservoirs: Connotation, design optimization and implementation. Pet Explor Dev 39(3):377–384
Roussel NP., Manchanda R, Sharma MM (2012). Implications of fracturing pressure data recorded during a horizontal completion on stage spacing design. SPE Hydraulic Fracturing Technology Conference
Sahai R, Miskimins JL, Olson KE (2014). Laboratory results of proppant transport in complex fracture systems. SPE Hydraulic Fracturing Technology Conference,
Sahai R, Moghanloo RG (2019) Proppant transport in complex fracture networks—a review. J Pet Sci Eng. https://doi.org/10.1016/j.petrol.2019.106199
Sun F, Du S, Zhao Y-P (2022) Fluctuation of fracturing curves indicates in-situ brittleness and reservoir fracturing characteristics in unconventional energy exploitation. Energy. https://doi.org/10.1016/j.energy.2022.124043
Taghichian A, Hashemalhoseini H, Zaman M, Yang Z-Y (2018) Geomechanical optimization of hydraulic fracturing in unconventional reservoirs: a semi-analytical approach. Int J Fract 213(2):107–138. https://doi.org/10.1007/s10704-018-0309-4
Wang J, Joseph DD, Patankar NA, Conway M, Barree RD (2003) Bi-power law correlations for sediment transport in pressure driven channel flows. Int J Multiph Flow 29(3):475–494

Wang M, Wilkins RW, Song G, Zhang L, Xu X, Li Z, Chen G (2015) Geochemical and geological characteristics of the Es3L lacustrine shale in the Bonan sag, Bohai Bay Basin, China. Int J Coal Geol 138:16–29

Wang J, Wang Z, Sun B, Gao Y, Wang X, Fu W (2019) Optimization design of hydraulic parameters for supercritical CO2 fracturing in unconventional gas reservoir. Fuel 235:795–809. https://doi.org/10.1016/j.fuel.2018.08.078

West I, Walton G (2023) Quantitative evaluation of the effects of input parameter heterogeneity on model behavior for bonded block models of laboratory rock specimens. Rock Mech Rock Eng 56(10):7129–7146. https://doi.org/10.1007/s00603-023-03248-9

Willingham, J., Tan, H., & Norman, L. (1993). Perforation friction pressure of fracturing fluid slurries. Low Permeability Reservoirs Symposium,

Wu F, Li D, Fan X, Liu J, Li X (2020) Analytical interpretation of hydraulic fracturing initiation pressure and breakdown pressure. J Nat Gas Sci Eng 76:103185. https://doi.org/10.1016/j.jngse.2020.103185

Xi Y, Lian W, Fan L, Tao Q, Guo X (2021) Research and engineering application of pre-stressed cementing technology for preventing micro-annulus caused by cyclic loading-unloading in deep shale gas horizontal wells. J Petrol Sci Eng 200:108359

Yang S-Q, Tian W-L, Ranjith PG, Liu X-R, Chen M, Cai W (2022) Three-dimensional failure behavior and cracking mechanism of rectangular solid sandstone containing a single fissure under triaxial compression. Rock Mech Bull 1(1):100008. https://doi.org/10.1016/j.rockmb.2022.100008

Yuan G, Che A, Shi Y (2023) Evaluation method of rock damage under uniaxial compression based on unit series-parallel electrical conductive model. Rock Mech Bull 2(4):100066. https://doi.org/10.1016/j.rockmb.2023.100066

Zhang D, Ranjith PG, Perera MSA (2016) The brittleness indices used in rock mechanics and their application in shale hydraulic fracturing: a review. J Pet Sci Eng 143:158–170. https://doi.org/10.1016/j.petrol.2016.02.011

Zhao B, Ratnakar R, Dindoruk B, Mohanty K (2020) A hybrid approach for the prediction of relative permeability using machine learning of experimental and numerical proxy SCAL data. SPE J. https://doi.org/10.2118/196022-pa

Zhong R, Johnson RL, Chen Z (2020) Using machine learning methods to identify coal pay zones from drilling and logging-while-drilling (LWD) data. SPE J. https://doi.org/10.2118/198288-pa

Zhu H, Tang X, Song Y, Li K, Xiao J, Dusseault MB, McLennan JD (2021) An infill well fracturing model and its microseismic events barrier effect: a case in fuling shale gas reservoir. SPE J 26(01):113–134

Zou C, Dong D, Wang S, Li J, Li X, Wang Y, Li D, Cheng K (2010) Geological characteristics and resource potential of shale gas in China [Article]. Pet Explor Dev 37(6):641–653. https://doi.org/10.1016/S1876-3804(11)60001-3